OPEN

ORIGINAL ARTICLE

Novel role of Engrailed 1 as a prosurvival transcription factor in basal-like breast cancer and engineering of interference peptides block its oncogenic function

AS Beltran[1], LM Graves[1] and P Blancafort[1,2]

Basal-like breast tumors are aggressive cancers associated with high proliferation and metastasis. Chemotherapy is currently the only treatment option; however, resistance often occurs resulting in recurrence and patient death. Some extremely aggressive cancers are also associated with hypoxia, inflammation and high leukocyte infiltration. Herein, we discovered that the neural-specific transcription factor, Engrailed 1 (EN1), is exclusively overexpressed in these tumors. Short hairpin RNA (shRNA)-mediated knockdown of EN1 triggered potent and selective cell death. In contrast, ectopic overexpression of EN1 in normal cells activated survival pathways and conferred resistance to chemotherapeutic agents. Exogenous expression of EN1 cDNA reprogrammed the breast epithelial cells toward a long-lived, neural-like phenotype displaying dopaminergic markers. Gene expression microarrays demonstrated that the EN1 cDNA altered transcription of a high number of inflammatory molecules, notably chemokines and chemokine receptors, which could mediate prosurvival pathways. To block EN1 function, we engineered synthetic interference peptides (iPeps) comprising the EN1-specific sequences that mediate essential protein-protein interactions necessary for EN1 function and an N-terminal cell-penetrating peptide/ nuclear localization sequence. These EN1-iPeps rapidly mediated a strong apoptotic response in tumor cells overexpressing EN1, with no toxicity to normal or non EN1-expressing cells. Delivery of EN1-iPeps into basal-like cancer cells significantly decreased the fifty percent inhibitory concentrations (IC$_{50}$) of chemotherapeutic drugs routinely used to treat breast cancer. Lastly, matrix-assisted laser desorption/ionization-time of flight mass spectrometry and immunoprecipitation assays demonstrated that EN1-iPeps captured targets involved in transcriptional and post-transcriptional regulation. Importantly, the EN1-iPeps bound the glutamyl-prolyl tRNA synthetase (EPRS) target, which has been associated with the transcript-specific translational control of inflammatory proteins and activation of amino-acid stress pathways. This work unveils EN1 as an activator of intrinsic inflammatory pathways associated with prosurvival in basal-like breast cancer. We further build upon these results and describe the engineering of iPeps targeting EN1 (EN1-iPeps) as a novel and selective therapeutic strategy to combat these lethal forms of breast cancer.

INTRODUCTION

Basal-like breast cancers lack expression of estrogen receptor (ER), progesterone receptor, and epidermal growth factor receptor-2 (HER2). The presence of stem cell-like signatures, frequent mutations of the tumor suppressor genes p53 and breast cancer 1, early onset (BRCA1) and genomic instability are major hallmarks of these tumors.[1–3] The response of these cancer types to first-line chemotherapy is often hindered by acquired resistance to treatment, recurrence and metastatic disease.[1,4,5] It has been recognized that survival and resistance of cancer stem cell-like cells to therapy is associated with a deregulated immunoresponse and/or excessive inflammation in the tumor microenvironment. High expression of inflammation (e.g. aberrant secretion of inflammatory cytokines and chemokines by breast cancer cells or stromal cells) and angiogenesis-related gene signatures are associated with poor prognosis.[2,6–11] Importantly, there is a lack of selective therapeutic agents to target these tumors and patients are left only with chemotherapy options.[12,13]

Recent large-scale studies of breast carcinomas have elucidated the fundamental role of transcription factors (TFs) as driving forces of oncogenesis in basal-like breast cancers.[13–18] Notably, many developmental homeodomain (HD) containing TFs (TF$_{HD}$s) are aberrantly expressed in cancer and are drivers of cancer initiation, disease recurrence and resistance to treatment.[18–20] However, despite their critical role in cancer, TFs have not been successfully targeted with conventional small molecules and have been considered 'undruggable'.

In this paper, we discovered the highly selective overexpression of neural-specific TFs, notably Engrailed 1 (EN1) in basal-like breast cancers. In humans, two paralogs, EN1 and EN2, control pattern formation during development of the central nervous system.[21] EN1 is expressed in neural progenitor cells and may expand and maintain the pool of dopaminergic neurons with prosurvival activity. A proposed function of EN1 in dopaminergic neurons is to promote survival and resistance to apoptotic insults, which preserves the longevity of these cells throughout adult life.[22]

[1]Department of Pharmacology, The University of North Carolina at Chapel Hill, Chapel Hill, NC, USA and [2]Cancer Epigenetics Group, School of Anatomy, Physiology and Human Biology, The University of Western Australia, Crawley, WA, Australia. Correspondence: Professor P Blancafort, Cancer Epigenetics Group, School of Anatomy, Physiology and Human Biology, The University of Western Australia, 35, Stirling Highway, Crawley, WA 6009, Australia.
E-mail: pilar.blancafort@uwa.edu.au

Mutations in the Engrailed genes cause neural cell degeneration induced by caspase-3-dependent apoptosis, which is one of the pathological features of Parkinson's disease.[21] Interestingly, in a recent study, the EN2 paralog has been associated with non-resectable prostate cancers.[23] The functional significance of the overexpression of Engrailed members in cancer, and more particularly, in basal breast cancer, is not known.

Our results outline the critical role of the neural-specific TF_{HD} EN1 in controlling inflammatory signals, survival and resistance to cell death in highly aggressive basal-like breast cancers having stem/progenitor cell characteristics. We also show that novel synthetic peptides or interference peptides (iPeps) comprising the highly conserved EN1-hexamotif sequence involved in protein–protein interactions, induce potent and selective apoptosis in highly resistant basal-like breast cancer cells. These peptides could be used as a novel selective therapeutic strategy to combat these forms of tumors for which no successful targeted treatment is available.

RESULTS

EN1 is overexpressed in the basal-like intrinsic subtype of breast cancer

To identify oncogenic TF_{HD}s in basal-like breast cancers, we first examined the mRNA expression of more than 200 TF_{HD}s using the UNC337 gene expression tumor database.[24] A total of 114 TF_{HD}s were significantly differentially expressed ($P < 0.05$) across tumor subtypes, with high representation of neural specific TF_{HD}s. The TF_{HD}s EN1 and EN2 were differentially expressed across the intrinsic subtypes (Figure 1a). However, EN1 had the highest and most selective enrichment in the basal-like breast cancers with $\sim$4-fold increased expression ($P = 4.65e^{-50}$) over normal-like, HER2, luminal A and B subtypes (Figure 1a and Supplementary Table S1).

To address whether EN1 expression in cancer patients correlated with poor survival, we took advantage of the MERGE 550 tumor database.[25] Cancer patients with higher EN1 expression had the lowest relapse-free survival ($P = 0.00399$), indicating an association of high EN1 expression with poor clinical outcome (Figure 1b). Conversely, EN2 expression did not exhibit a significant impact on overall survival (data not shown).

To validate the gene expression microarray data, we quantified EN1 mRNA levels in a panel of breast cancer cell lines encompassing all of the six different intrinsic subtypes of breast cancer. In accordance with the microarray data, the EN1 gene was highly expressed in basal-like cell lines with highest expression in SUM149PT, and absent in luminal lines, such as MCF-7 and normal breast epithelial cells (human mammary epithelial cells (HUMEC); Figure 1c). The EN1 protein expression levels in the cell lines were in accordance with mRNA levels, as assessed by immunofluorescence. EN1 protein expression was detected in a sub-population of cells, which displayed mostly strong nuclear staining (Figure 1d).

The EN1 expression in triple-negative tumor specimens with basal-like features (e.g. high-grade ductal invasive carcinomas) revealed some cytoplasmic and mostly nuclear localization. Similar to the detection pattern in the cell lines, the EN1 staining in the tissue sections was heterogeneous. In contrast, none of the hormone receptor-positive tumors or normal-like tissue examined (e.g. breast tissue from a mammoplastic reduction) revealed any detectable EN1 staining (Figure 1e). Basal-like tumors are associated with germ-line mutations in the *breast cancer 1, early onset* (BRCA1) and *p53* genes.[3,14,16,26] We next took advantage of cell lines derived from genetically engineered mouse models to interrogate the expression of EN1 in these samples. Interestingly, high EN1 mRNA expression was detected in two cell lines possessing stem cell-like characteristics: the T11 line, isolated from p53-deficient mice,[27,28] and the BRCA1-A1.8 line, isolated from a BRCA1 mutant mice[29–31] (Supplementary Figure S1). In summary, these results suggest that EN1 was overexpressed in a sub-population of triple-negative breast cancer cells with basal-like features.

EN1 expression confers survival features to breast cells

To decipher the role of EN1 in breast cancer cells, we used lentivirally delivered short hairpin RNAs (shRNAs) to knockdown EN1 expression in the basal cancer cell line SUM149PT cells. Forty-eight hours after transduction, the EN1-specific shRNAs (but not control shRNA) triggered a strong cell death (Figure 2a) that was due to induction of apoptosis, as assessed by caspase-3 (Figure 2c) and poly(ADP-ribose) polymerase-cleavage assays (Figure 2d). In contrast, transfection of EN1-shRNAs in the low-EN1-expressing MDA-MB-231 cell line did not reveal any significant changes in caspase-3 activity relative to control (Supplementary Figure S2). The above results indicated that shRNA-mediated knockdown of EN1 selectively impacted survival pathways in cell lines expressing high levels of EN1.

In the neural system, it has been proposed that EN1 protects neurons from mitochondrial complex I insults.[22] Likewise, we investigated whether EN1 could have a similar role in the basal-like breast cancer cell lines. EN1 cDNA was overexpressed in SUM149PT cells using a lentiviral vector, and the transduced cells were treated with increasing concentrations of rotenone, a mitochondrial complex I toxin, and taxol, a microtubule-destabilizing agent. Transfection of EN1 cDNA increased EN1 protein expression (Supplementary Figure S3a) and significantly increased the fifty percent inhibitory concentrations (IC_{50}) for rotenone (from 1.078 to 19.61 μM; Figure 2e) and taxol (from 7.24 to 47.81 μM; Figure 2f) relative to control transduced cells. In fact, EN1 overexpression in breast cancer cells did not result in enhanced cell proliferation (Supplementary Figures S3b and c) or tumorigenic potential, as shown by soft agar colony formation assays (Supplementary Figures S3d and e). Similarly, the over-expression of the EN1 cDNA in other cell lines, including cell lines not expressing the EN1 gene, such as MDA-MB-231, also resulted in an increased resistance to neurotoxins and other chemotherapeutic insults (data not shown).

Lastly, we examined potential downstream transcriptional targets of EN1 by performing genome-wide gene expression microarray analysis of SUM149PT cells overexpressing the EN1 cDNA and control vector (Supplementary Table S2). We specifically chose SUM149PT cells as they represent one of the few cell lines isolated from inflammatory breast cancer.[32,33] Gene ontology analysis of differentially regulated genes revealed the upregulation of pathways involved in inflammation, cytokine and chemokine activity and angiogenesis (e.g. CXCL11, CD69, IL23A, interleukin 1 receptor-like 1/2, CXCL6, interleukin 8 and vascular epithelial growth factor A; Supplementary Table S3). These results suggest a potential link between EN1 expression and inflammatory breast cancer via the activation of downstream chemokine signaling pathways.

To better understand the function of EN1 in the pathology of breast cancer, the EN1 cDNA was overexpressed using a lentiviral vector in primary preparations of HUMECs generated from reduction mammoplasties. HUMEC cells were transduced with either EN1 cDNA or a control enhanced green fluorescent protein (EGFP), and 72 h after transduction, these cells were seeded in fibroblast feeder cultures with human embryonic stem cell medium, conditions that favor the propagation of mammary stem/progenitor cells.[20] Although the primary HUMEC control cells could not be maintained in culture or passaged after 3 weeks, the EN1-overexpressing cells survived for more than 6 months in culture with a very low division rate (Figure 2g). Furthermore, the HUMEC-EN1 cells differentiated into neural-like cells within a period of 3 weeks when placed in a neural differentiation medium. As EN1 is normally expressed in mesencephalic dopaminergic neurons, the expression of mesencephalic dopaminergic-specific
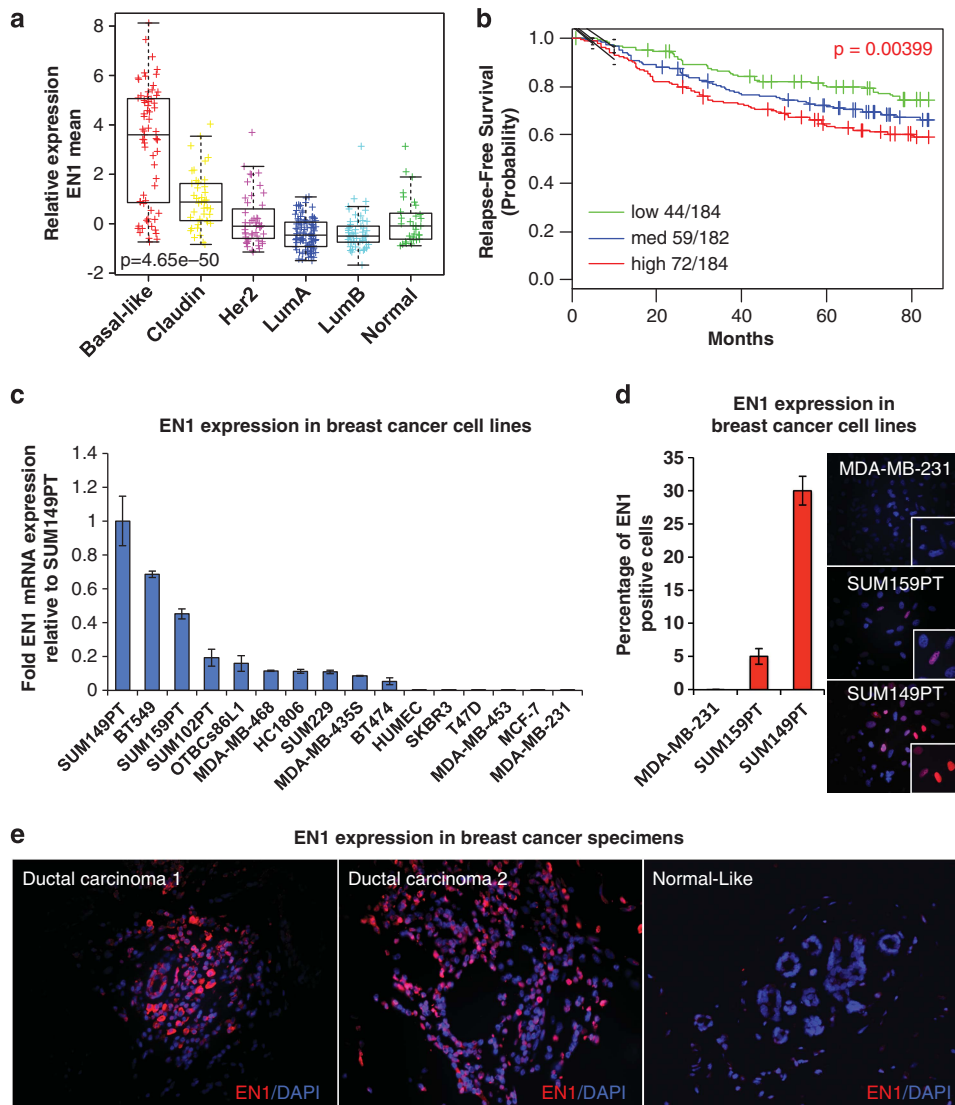
Figure 1. Engrailed 1 (*EN1*) is expressed in basal-like breast cancer. (**a**) Box and whisker plot for the mean expression of *EN1* across the intrinsic molecular subtypes of breast cancer on the UNC337 breast cancer patient database. *P*-values were calculated by comparing gene expression means across all subtypes. BL, basal-like; CL, claudin-low; HER, HERB-b2 enriched; LA, luminal A; LB, luminal B; NL, normal-like. (**b**) Kaplan–Meier (KM) plot of relapse-free survival indicates that EN1 positivity in basal-like breast carcinoma from the Merge 550 tumor database is correlated with poor survival (*P* = 0.00399) in high expressing tumors. (**c**) *EN1* mRNA levels by qRT–PCR in a panel of breast cancer cell lines. Data were normalized to SUM149PT cell line and represents the average and standard deviation (s.d.) of three independent experiments. (**d**) EN1 immunofluorescence detection in representative high (SUM149PT, SUM159PT) and low (MDA-MB-231) EN1-expressing cell lines. EN1 (red) was labeled with Alexa 594 and nucleus (blue) with 4′,6-diamidino-2-phenylindole (DAPI). A representative picture is shown. A quantification of the percentage of EN1-positive cells for each cell line is indicated in the histogram. (**e**) EN1 immunofluorescence detection in representative clinical specimens: two triple-negative ductal invasive carcinomas and a normal-like breast preparation generated from a mammoplasty reduction.

markers such as tyrosine hydroxylase, vesicular monoamine transporter 2, dopamine transporter, neuron-specific class III β-tubulin (Tuj1) and aldehyde dehydrogenase 1 family member A1 was assessed by immunofluorescence. The HUMEC-*EN1* cells displayed strong EN1 nuclear and faint cytoplasmic staining, the later overlapping with Tuj1 expression (Figure 2g, top right panel). Interestingly, these cells also displayed strong dopamine transporter and vesicular monoamine transporter expression (Figure 2g, lower right panel) as well as tyrosine hydroxylase and aldehyde dehydrogenase 1 family member A1 (Figure 2g, lower left panel). Despite the increase in dopaminergic markers, the HUMEC-*EN1* cells failed to display typical neuronal excitability as assessed by whole-cell electrophysiological recording (data non shown), suggesting that more than a single TF is necessary for full

conversion to functional dopaminergic neurons. Alternatively, transduction of EN1 could give rise to dopaminergic neurons at a very low frequency. Overall, these results suggest that expression of *EN1* in breast cells could activate developmental pathways similar to those of dopaminergic neurons, providing cells a means to sustain survival against apoptotic stimuli.

Targeting EN1 with iPeps

To inhibit the function of *EN1* as a TF in basal-like breast cells, we engineered synthetic iPeps comprising the EN1-specific hexamotif and flanking protein sequences from the N terminus of the HD. Synthetic peptides comprising either the murine EN2 or HOXA9 hexamotifs have been previously shown to compete *in vitro* with
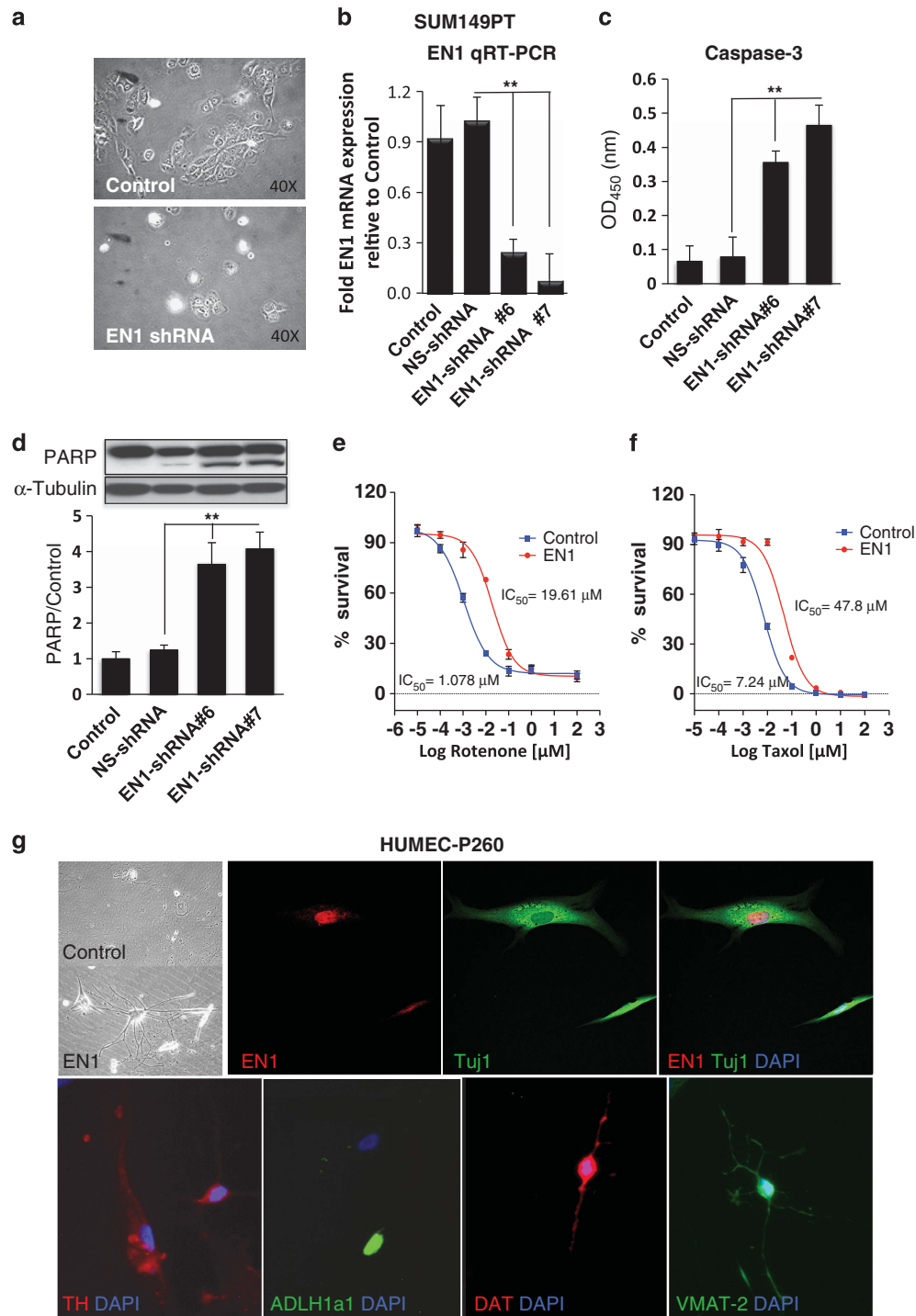
Figure 2. *EN1* confers survival features to breast epithelial cells. (**a**) Representative light microscopy picture of SU149PT cells after shRNA-mediated knockdown of *EN1* at ×40 magnification. Cells were transduced with a nonspecific shRNA (upper panel) or EN1-specific shRNAs (shRNA nos. 6 and 7, lower panel). (**b**) *EN1* mRNA levels assessed by qRT–PCR in shRNA-transduced cells. (**c**) Caspase-3 activity after shRNA-mediated knockdown of *EN1*. (**d**) Upper panel: representative western blot of poly (ADP-ribose) polymerase (PARP) cleavage levels in cells after shRNA-mediated knockdown of *EN1*. Tubulin was used as loading control. Data in (**b**–**d**) were normalized to control (non-transduced cells); the average error and standard deviation (s.d.) of three independent experiments is indicated. Statistical significance was analyzed using the Student's *t*-test (******$P < 0.01$). (**e**) Dose–response plots of stable SUM149PT cell lines overexpressing the *EN1* cDNA or *EGFP* (control cells) treated with increasing concentrations of taxol and rotenone for 72 h. (**f**) Cell viability was assessed by CTG assay and the percentage of survival (%) was normalized to the vehicle-treated cells. Determination of IC_{50} was performed using a non-linear regression method (curve fit) with the GraphPad software (San Diego, CA, USA). (**g**) Light and fluorescent imaging of HUMEC-P260 overexpressing *EN1*. Light imaging pictures show cells transduced with a control (empty vector) and *EN1* cDNA. Fluorescent images show the detection of neural-specific markers (in red); tyrosine hydroxylase (TH), vesicular monoamine transporter 2 (VMAT-2), dopamine transporter (DAT), neuron-specific class III beta-tubulin (Tuj1) and aldehyde dehydrogenase 1 family member A1 (ALDH1A1). Nucleus was stained with 4′,6-diamidino-2-phenylindole (DAPI). Pictures were taken at ×40.

the EN2-PBX1 or HOXA9-PBX1 complexes and disrupt TF_{HD}–TF_{HD} interactions necessary for cooperative DNA binding.[34] As shown in Figure 3a, the interaction between PBX1 and HOXA9 is mediated by a hexamotif-like sequence. A similar hexamotif sequence (WPAWVY) is present in human EN1 protein, and located at the N terminus of the HD. We reasoned that the delivery of a synthetic peptide comprising the human EN1 hexamotif and flanking sequences would phenocopy the effect of the EN1-specific shRNAs and induce selective cell death in the basal-like breast cancer cells.

Sequence comparison showed that the hexamotif WPAWVY and the CTRYSDRPS C-terminal sequence of the human EN1 protein were highly conserved among vertebrate and invertebrate species (Figure 3b). A specific cell-penetrating peptide (sequence KKKRKV) that acts as nuclear localization sequence was included in the N terminus of the iPep sequence variants (Figure 3c). We chose this specific nuclear localization sequence/cell-penetrating peptide sequence as it has been shown to be effective in

mediating penetration of peptide cargos containing hydrophobic residues, such as W and Y.[35]

The EN1-iPeps and iPep controls were first tested in SUM149PT cells carrying high *EN1* expression. Cells were treated with a full-length 29-mer peptide (iPep624) comprising the N terminal, less conserved amino-acid sequences, the hexamotif, and the C-terminal tail. As a control, we generated the iPep624ΔHEX in which the hexamotif was mutated from the wild-type (wt) WPAWVY to the GAAGAG sequence. These mutations were expected to dramatically abolish the activity of the peptide. Both peptides were included in the culture medium of the basal cancer cells in increasing (0–100 μM) concentrations and incubated for 8 h at 37 °C. Treated cells were first analyzed using the Cell Titer Glo (CTG) assay, which monitors metabolic viability. Although cells treated with the iPep624ΔHEX did not show significant changes in cell viability, even at 100 μM, the cells treated with iPep624 showed strongly reduced viability in a dose-dependent manner with an IC_{50} of 17.5 μM (Figure 3d). This IC_{50} value is in the range of
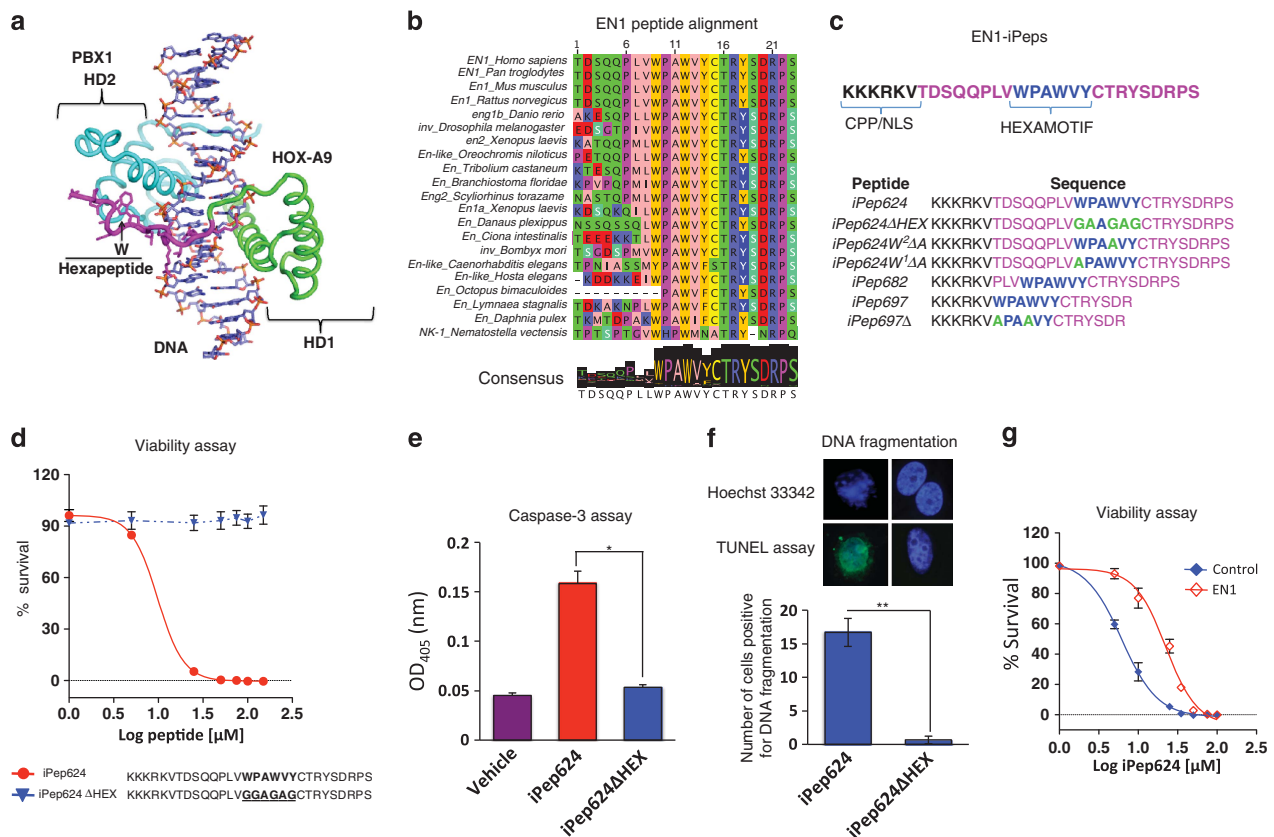

Figure 3. Design of an EN1-iPep. (**a**) Molecular model of HOXA9 and PBX1 tertiary complex formation with the DNA (PDB: 1PUF). HOXA9 (hexapeptide 'donor') is shown in green; PBX ('partner') in blue. The N-terminal peptide of HOXA9 (magenta) is essential to make contact with the DNA minor groove, as well as to stabilize the binding of HOXA9 with PBX1. The conserved tryptophan residue (W, arrow) is shown within the hexapeptide and it is responsible for anchoring the loop in PBX1. HD, homeodomain. (**b**) A multiple alignment of the EN1-iPeps across species, with the consensus sequence of the iPep indicated below. (**c**) Design of the EN1-iPep composed of 23 amino acids; the hexamotif is shown in blue and the six amino-acid cell penetration/nuclear localization sequence (CPP/NLS) is indicated in black. (**d**) Dose–response curve showing cell viability against increasing concentrations of active iPep624 or mutant iPep624ΔHEX peptide in SUM149PT cells. Cells were treated for 8 h and cell viability assessed by CTG assay. Percentage of survival (%) was normalized to the vehicle-treated cells. Determination of IC_{50} was performed using a nonlinear regression method (curve fit) with the GraphPad software (San Diego, CA, USA). (**e**) Caspase-3 activity in SUM149PT cells measured after 48 h of iPep624 or iPep624ΔHEX treatment. Average and s.d. of three independent experiments is indicated. Statistical significance was analyzed using the Student's t-test (*$P < 0.01$). (**f**) iPep624 but not iPep624ΔHEX induce DNA fragmentation in SUM149PT breast cancer cells, as assessed by a Hoechst 33342 staining and a terminal deoxynucleotidyl transferase dUTP nick-end labeling (TUNEL) assay in the iPep-treated cells. Pictures on the top show the detailed morphology of the nuclei after 8 h of iPep treatment. Histogram represents the quantification of the number of cells positive for DNA fragmentation (TUNEL-positive cells) per field of view at × 40 magnification. Average and s.d. of three independent experiments is indicated. Statistical significance was analyzed using the Student t-test (**$P < 0.001$). (**g**) Dose–response plots of stable SUM149PT cell lines overexpressing the *EN1* cDNA or EGFP (control cells) treated with increasing concentrations of the iPep624 for 72 h. Cell viability was assessed by CTG assay and the percentage of survival (%) was normalized to the control-treated cells. Determination of IC_{50} was performed using a nonlinear regression method.

concentrations observed with other peptides delivered with cell-penetrating peptides.[35] Both caspase-3 activity (Figure 3e) and the number of apoptotic nuclei undergoing DNA fragmentation (Figure 3f) were significantly higher in the iPep624-treated cells as compared with non-treated or iPep624ΔHEX-treated cells. Furthermore, the cell viability defect provoked by iPep624 was rescued by ectopic transfection of the *EN1* cDNA (Figure 3g), suggesting that with higher *EN1* expression, more peptide is needed to inhibit its function. These experiments indicate that the apoptotic response induced by EN1-iPep624 was specific and dependent on the expression of *EN1*.

To rule out the possibility that differences in apoptosis were the consequence of differential internalization and/or intracellular distribution of the peptides, real-time peptide internalization studies were performed. Both active and mutant iPeps were coupled to a C-terminal fluorescein molecule and delivered into SUM149PT cells. Cells were imaged every 2 min over a 60-min period using a confocal microscope. The total fluorescence per image was measured as the total number of pixels captured at 488 nm. We found that both active and inactive iPeps entered in the cytoplasm in < 2 min and reached a plateau with saturating levels of fluorescence attained after ~ 40 min (Figures 4a and b; Supplementary Figure. S4).

EN1-iPeps selectively target basal-like breast cancer lines expressing *EN1*

To test the specificity of the EN1-iPep in cell lines expressing *EN1*, we delivered the iPeps into a panel of breast cancer cell lines expressing different amounts of EN1. The iPep624 selectively decreased cell viability of basal-like EN1-expressing cell lines such as SUM149PT, SUM159PT, SUM102 and SUM229 but had no effect on cell viability in low or non-expressing EN1 cell lines, such as the MCF-7, MDA-MB-231 and HUMEC cell lines (Figure 5a). In addition, the mutant iPep624ΔHEX peptide did not significantly affect cell viability of any of the breast cancer cell lines at the maximum tested concentrations (100 μM) (Figure 5b).

To investigate the requirement of the two W residues in the activity of the peptide, mutant iPeps were generated with either the first (iPep624W^{1}ΔA) or the second tryptophan (iPep624W^{2}ΔA) mutated to alanine and delivered into SUM149PT cells. These mutations were expected to disrupt the structure of the hydrophobic pocket necessary for EN1 to cooperatively bind other binding partners in the cell. Both W mutants retained activity but significantly increased the IC$_{50}$ as compared with the wt iPep624. Molecular modeling analysis of the alanine mutations suggests a wide hydrophobic pocket in the iPep624W^{2}ΔA and a narrow interacting interface in iPep624W^{1}ΔA (Figure 5c, right). These results highlight the structural selectivity of the peptide and the requirement of the W residues in the EN1 hexamotif for inhibitory activity.

Next, we mapped the minimal EN1-iPep sequence retaining cell growth inhibitory activity *in vitro*. We generated peptide EN1-iPep682 (Figure 3c) lacking the less evolutionarily conserved five N-terminal residues, and two C-terminal residues of the parent peptide iPep624. The iPep682 was even more effective than the parent full-length iPep624 peptide decreasing the IC$_{50}$ from 17.5 to 12.5 μM (Figure 5d). Interestingly, a 13-mer peptide lacking all the N-terminal residues upstream of the hexamotif (iPep697) was less active than the wt EN1-p624 peptide (Figure 5d), suggesting that the N-terminal arm of the peptide immediately adjacent to the hexamotif (comprising the proline–valine–leucine residues) also provides sequence-specific determinants essential for inhibitory activity.

Lastly, we investigated the capability of the active EN1-iPep (iPep682) to sensitize breast cancer cells to Food and Drug Administration-approved drugs, such as taxol and 5-fluorouracil. SUM149PT cells were particularly resistant to these agents with an IC$_{50}$ of 7.6 μM for taxol (Figure 5e) and 610 μM for 5-fluorouracil (Figure 5f) after 48 h of treatment with these agents. However, cells treated for 48 h with drug and for 8 h with low concentration of the iPep682 (500 nM) significantly decreased the IC$_{50}$ of taxol from 7.6 μM to 49 nM (Figure 5e), and 5-fluorouracil from 610 to 29.47 μM (Figure 5f). These experiments demonstrate that the low doses of iPeps could further sensitize highly resistant breast cancer cells to chemotherapy agents.

EN1-iPeps capture intracellular targets involved in control of translation and transcriptional regulation

To investigate the binding partners of the iPeps in cancer cells, we carried out affinity capture immunoprecipitation experiments using the biotinylated active iPep624 as bait, and the iPep624Δ HEX as negative control. We used total protein extracts from SUM149PT cells to capture endogenous proteins able to bind these peptides *in vitro*. Elutes were loaded on a one-dimensional-sodium dodecyl sulfate–polyacrylamide gel electrophoresis gel to visualize the enrichment of individual proteins. As shown in Figure 6a, a protein of ~ 170 kDa was differentially enriched in the iPep624-elutes relative to iPep624ΔHEX. Protein identification using matrix-assisted laser desorption/ionization-time of flight/time of flight mass spectrometry revealed a highly significant score for the glutamyl-prolyl tRNA synthetase (EPRS), an enzyme
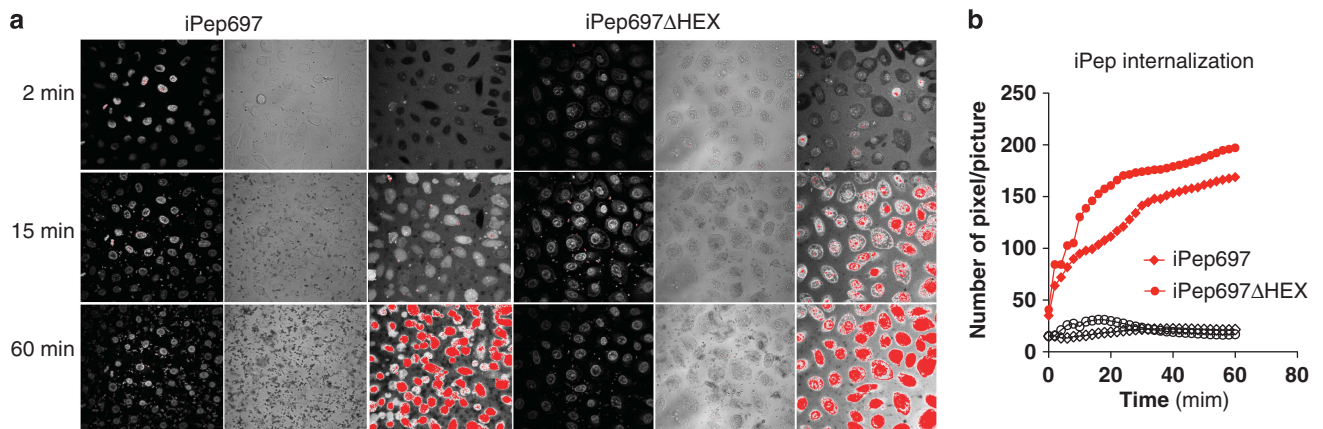

Figure 4. Internalization kinetics of fluorescently labeled iPeps in SUM149PT cells. (**a**) Real-time imaging of the EN1-specific iPep697 and the mutant iPep697ΔHEX conjugated with a C-terminal fluorescein by confocal microscopy. Cells were treated with 15 μM of iPep and imaged every 2 min during 1 h. Images at 2, 15 and 60 min were taken at × 40 magnification. (**b**) Quantification of pixels during the real-time imaging of the iPep697 and iPep697ΔHEX in either green or blue channel over a 60-min period.
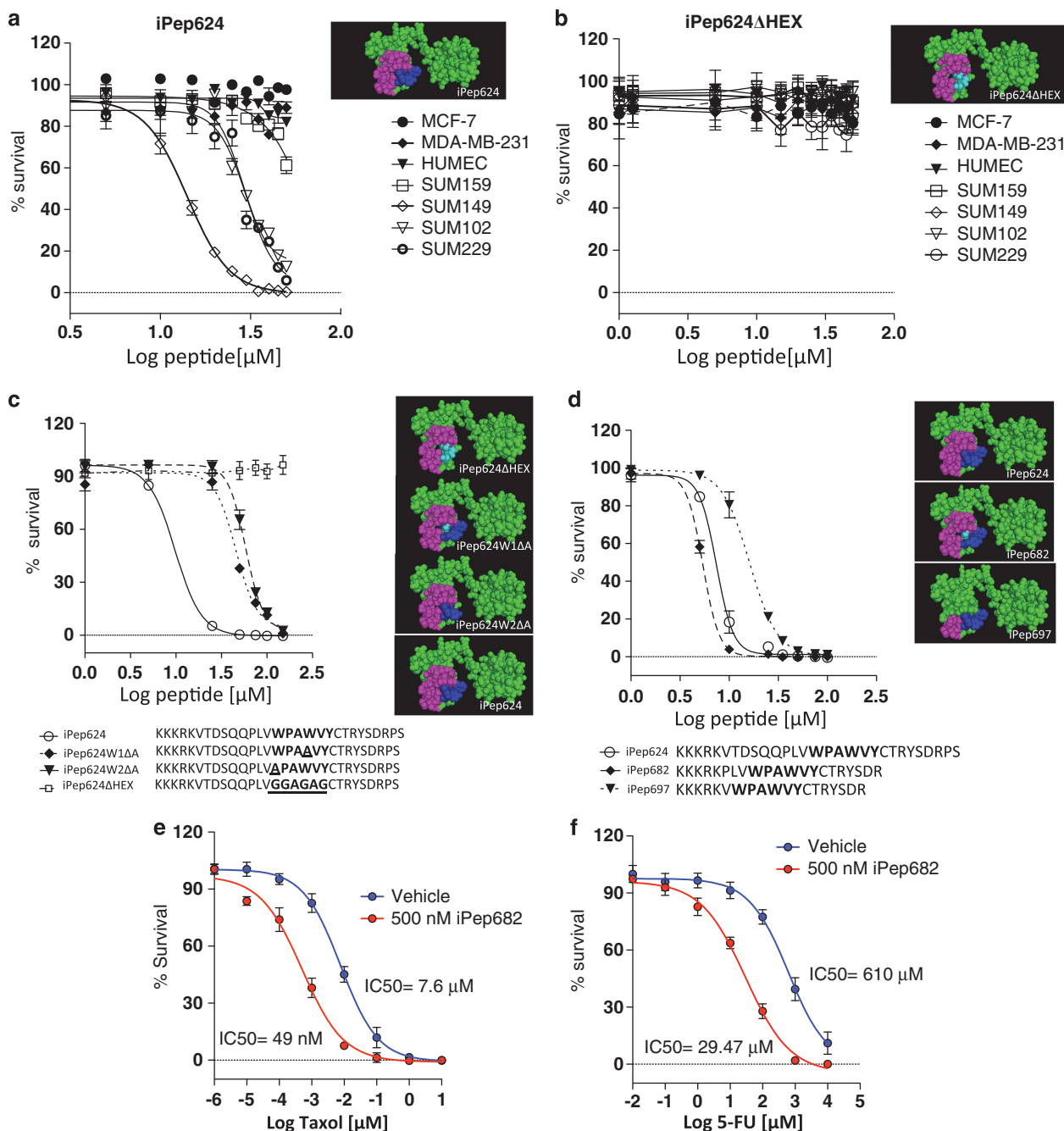
Figure 5. EN1-iPeps selectively target basal-like breast cancer lines expressing *EN1*. (**a** and **b**) Dose–response plots showing cell viability against increasing concentrations of iPep624 (**a**) or iPep624ΔHEX (**b**), hexamotif WPAWVY mutated to GGAGAG in a panel of breast cancer cell lines. Cells were treated with the iPep for 8 h and cell viability assessed by CTG assays. Percentage of survival (%) was normalized to the vehicle-treated cells. Determination of IC_{50} was performed using a nonlinear regression method. (**c**) Dose–response plot of SUM149PT cells treated with increasing concentrations of iPep624, iPep624W1ΔA (first tryptophan mutated to alanine), iPep624W2ΔA (second tryptophan mutated to alanine) and iPep624ΔHEX (hexamotif WPAWVY mutated to GGAGAG). Percentage of survival and IC_{50}s were calculated as described above. (**d**) Dose–response plot of SUM149PT cell treated the iPep624 (29-mer), iPep682 (22-mer) and iPep697 (19-mer). Percentage of survival and IC_{50}s were calculated as describe above. (**e**) Dose–response plots of SUM149PT treated with 500 nM iPep682 and increasing concentrations of Taxol or 5-fluouracil (5-FU, **f**). Cells were challenged with Taxol or 5-FU for 60 h and then treated with the iPep682 for 8 additional hours. Cell viability was assessed by a Cell Titter Glo (CTG) assay and percentage of survival (%) was normalized to the fixed iPep concentration. The EN1-specific iPeps were modeled and visualized using PyMOL Molecular Graphics modeling and visualization software.

that controls transcript-specific mRNA and protein synthesis, particularly of inflammatory proteins and downstream effectors of the amino-acid stress pathway.[36] The preferential binding interaction EPRS with iPep624 over control peptide was validated by immunoprecipitation and immunoblotting (Figure 6b). In addition, overexpression of *EN1* cDNA into two different breast cell lines confirmed the interaction of the full-length EN1 with the endogenous EPRS inside the cells (Figure 6c). To ascertain whether some downstream well-known effectors of EPRS were also differentially regulated by the iPeps, we performed real-time
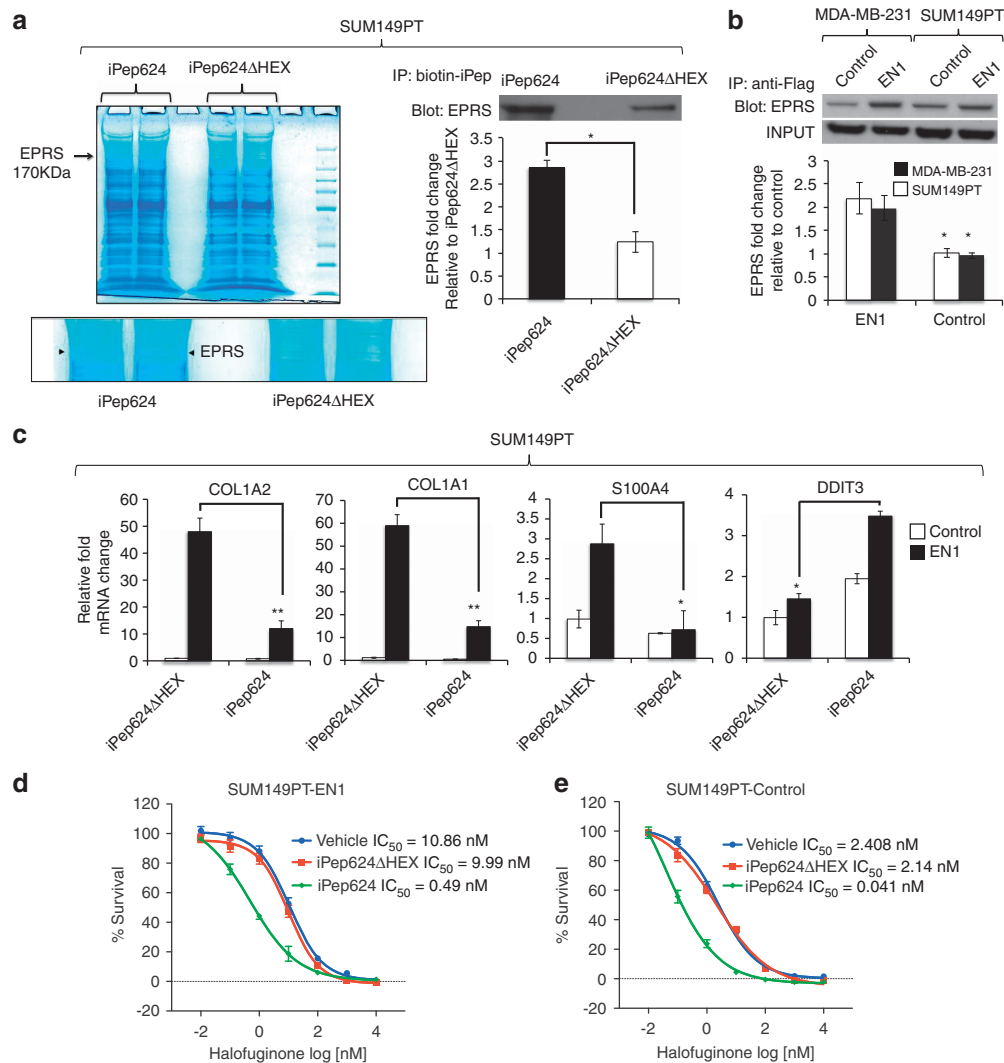
Figure 6. EN1-Ipeps binds the endogenous EPRS target and regulates downstream EPRS effectors in breast cancer cells. (a) EN1-iPep624 captures and binds EPRS from total extracts of SUM149-PT cells. Left: SDS–PAGE gel outlining the bands differentially bound to iPep624 and not in control iPep624ΔHEX. Experiments were carried out in duplicate. Extracts of SUM149PT cells were immunoprecipitated using biotinylated iPep624 or iPep624ΔHEX peptides as bait, and elutes applied to a SDS–PAGE (10% acrylamide). Gels were stained with Coomassie brilliant blue and the select band unique to the active iPep624 immunoprecipitates (∼170 kDa, arrow) was excised, digested with trypsin and analyzed using a matrix-assisted laser desorption/ionization-time of flight/time of flight mass spectrometer (AB Sciex; 4800 Plus). The band was identified as EPRS. Right: Affinity-capture immunoprecipitation and western blot detection of EPRS using biotinylated iPeps as bait, and total extracts of SUM149-PT cells. Same input loading of extract is shown in the SDS–PAGE gel on the left. The enrichment of the immunoprecipitated products was quantitated using Image J software and normalized to inactive iPep624ΔHEX peptide. The immunoprecipitations were carried out at least three times and averages and s.e.'s between experiments are indicated (*P < 0.01). (b) Full-length EN1 binds the endogenous EPRS in MDA-MB-231 and SUM149PT cells. Total extracts of MDA-MB-231 and SUM149PT expressing either a full-length EN1 cDNA engineered with a N-terminal FLAG tag or an empty-vector control were processed by immunoprecipitation with an anti-FLAG antibody. Immunoprecipitated complexes were blotted with an EPRS-specific antibody to detect endogenous EPRS. The same amount of loaded extracts (INPUT) is shown with anti-tubulin as endogenous control. The enrichment of the immunoprecipitated products was determined by quantification of the bands by densitometry as described above, and data were normalized to iPep624ΔHEX control. The immunoprecipitations were independently performed at least three times and averages and standard errors between experiments are indicated (*P < 0.01). (c) EN1-iPep624 regulates well-known downstream effectors of EPRS. SUM149PT cells overexpressing either the EN1-cDNA or an empty vector control (control) were challenged to 15 μM of active EN1-iPep624 or inactive iPep624ΔHEX control peptide. Cells were processed for qPCR expression analysis to detect mRNA levels. Fold-change mRNA regulation was normalized for each detector to iPep624ΔHEX control (*P < 0.01; **P < 0.001). (d) EN1-iPep624 but not iPep624ΔHEX control sensitizes SUM149PT cells to the EPRS inhibitor halofuginone. EN1-cDNA and control vector overexpressing cells were treated with 500 nM of iPep and challenged with increasing concentrations of halofuginone for a total period of 48 h. Cell viability was determined by a CTG assay and IC50 concentrations determined as described in Figure 5.

polymerase chain reaction (PCR) to detect mRNA levels of *COLA1*, *COLA2*, *S1004A* and *DDIT3* (*CHOP*). We chose these targets as they are transcriptionally modulated by both small interfering RNA knockdown and pharmacological inhibition of EPRS by halofuginone. Halofuginone is a februgirine derivative of a natural

product used to treat cancer, malaria, fibrosis and inflammation.[36] *COLA1* and *COLA2* encode collagen proteins highly enriched by the amino acid proline and *S1004A* is a protein involved in metastasis and fibrosis. These targets have been shown to be differentially downregulated upon inhibition of EPRS. In contrast,

the amino-acid stress factor *DDIT3* is stimulated upon EPRS inhibition.[36] To investigate if these targets were modulated by the *EN1* cDNA and the EN1-iPeps, both control and EN1-overexpressing SUM149PT cells were challenged with active iPep624 or inactive iPep624ΔHEX and processed by real-time PCR. As expected, the targets *COLA1*, *COLA2* and *S1004A* were significantly downregulated in the EN1-overexpressing cells, and this downregulation was significanctly inhibited by the addition of active peptide. Conversely, the *DDIT3* target was significantly upregulated in EN1-overexpressing cells by the active iPep over control, in accordance with the specific pharmacological inhibition of EPRS by halofuginone.[36] Interestingly, treatment of SUM149PT cells with halofuginone, iPep624 (Figure 6d) or an EPRS-specific shRNA (data not shown) induced potent breast cancer cell death. Cotreatment of SUM149PT cells with iPep624, but not peptide control, sensitized the basal-like breast cancer cells to halofuginone (Figures 6d–e). Consistent with EN1 providing resistance to cell death, the combination of iPep624 and halofuginone was more effective in SUM149PT-control cells than the SUM149PT-EN1-expressing cells (0.041 versus 0.49 nM). Overall, these studies indicated that EPRS was bound by iPep624 and full-length EN1 in the cancer cells. Moreover, these results suggested that pharmacological inhibition of EPRS using iPeps or the combination of iPeps with specific inhibitors of EPRS, (halofuginone), was extremely effective for inhibition of basal-like breast cancer cell survival.

Lastly, we examined whether iPep624 could also interact with other $TF_{HD}s$ expressed in basal-like cancers, using immunoprecipitation and western blotting. We observed specific interactions of iPep624, but not control peptide, with the PBX family members, notably PBX1 and PAX6 (Supplementary Figure S5). PBX1 and PAX6 are well-known partners of Engrailed proteins in other cell systems, particularly in dopaminergic neurons.[37] We also discovered a specific interaction between EN1-iPep and the TF_{HD} Distaless 6 (DLX6), which was found expressed at very high levels in the basal cancers in our tumor gene expression database (Supplementary Table S1). DLX6 expression has been associated with organ-specific breast cancer metastases.[38] In summary, our data demonstrate that the EN1-iPeps are able to inhibit the oncogenic function of *EN1* in basal cancer cells expressing *EN1*, by interacting with multiple intracellular partners involved in transcriptional regulation (particularly in the neural system) and further suggest that EPRS could be a novel downstream effector of EN1.

DISCUSSION

In our effort to discover biomarkers suitable for specific targeting of basal-like breast cancer, we explored a new approach by searching the breast cancer DNA microarray database for TFs specifically upregulated in the basal breast cancer subtype. Our analyses demonstrated that *EN1* was selectively and highly expressed in basal-like breast cancers with an average of fourfold over all the other subtypes. These results are in agreement with a recent study in salivary gland adenoid cystic carcinoma where high EN1 was correlated with histologic tumor grade, tumor location and patient outcome.[39]

Interestingly, one of the functions of EN1 is to modulate mitochondrial signals in adult dopaminergic neurons that protect cell survival pathways. We sought to determine if EN1 has a similar role in models of basal-like breast cancer, which frequently respond to treatment but later acquire drug resistance. Knocking down *EN1* expression in basal-like breast cancer cells with a specific shRNA resulted in a strong apoptotic response as demonstrated by caspase-3 activation assays. These results are similar to those observed in mouse mesencephalic dopaminergic neurons, where an shRNA targeting the Engrailed genes activated caspase-3 and induced apoptosis in < 24 h.[40] Interestingly, EN1-overexpressing cells treated with rotenone, a mitochondrial complex I inhibitor, or taxol, a microtubule inhibitor, were more resistant to these chemotherapy

regimens than control-transduced cells. Thus, these results suggest that EN1 conferred protective features to breast cancer cells, similar to that observed in mesencephalic dopaminergic neurons.[22]

On the basis of these and other studies, we propose that basal-like tumor phenotype is the result of the development of unique survival pathways, some of which are expressed in long-lived neural-stem cells, and *EN1* maintains those traits. The discovery of EN1 as a potential biomarker for basal-like breast cancer represents an opportunity to target selectively the tumor cells that are at the origin of dormancy, and resistance to anti-cancer treatments. In the future, the expression of *EN1* needs to be determined in a larger number of triple-negative breast cancer samples, with known clinical variables, particularly BRCA1 status, comprising the tissue before and after acquired resistance or relapse (e.g. drug resistant metastatic tissues), to ascertain whether EN1 is a marker involved in acquired resistance beyond the initial sensitivity to therapy in cancer patients.

Our gene expression microarray analysis of *EN1*-overexpressing cells show differential regulation of multiple cytokines and other immunomodulators normally engaged in inflammatory responses, T-cell immunity, fibrosis and angiogenesis (e.g. interleukin 8, interleukin 1 receptor-like 1, CD69, fibronectin 1 and vascular epithelial growth factor A). Cytokines and chemokines have emerged as one of the main mechanisms by which inflammation promotes breast cancer development, therapy-resistance and metastasis.[6,7] Recent gene expression data suggest that the immune response profile and inflammatory signature of breast cancers provide prognosis information and may predict response to treatment.[8,11] This inflammation gene expression signature demonstrates aberrant overexpression of cytokines, chemokines, vascular epithelial growth factor A, fibronectin 1 and other immunomodulators, notably T-cell tumor immunity.[8,11] Similarly, cytokines and cytokine receptors are also expressed by dopaminergic neurons and have been associated with prosurvival, oxidative stress and resistance to cell death.[41–43] The high *EN1*-expressing cell line SUM149PT was isolated from inflammatory breast cancer,[32] suggesting a novel, potential link between *EN1* expression, inflammation and basal-like cancer.

To inhibit the function of *EN1* as a TF in basal breast cells, we generated iPeps, which encompassed the sequence known to mediate protein–protein interactions between $TF_{HD}s$.[44–46] We designed iPep624 using the structural information from the HOX-PBX interactions.[46] We have shown that the active iPeps comprising the wt EN1 hexamotif selectively targeted cells expressing *EN1*, potentially by interfering or competing with EN1 partners in the cancer cell. In a similar study by Morgan and co-workers,[47–50] short peptides derived from the HOX-family of TFs were able to abolish cancer cell growth in leukemia and other cancer models.[23,47–50] These studies also demonstrated that peptides derived from HOX proteins were able to bind PBX in the cancer cells by competing with the endogenous HOX TFs. Interestingly, our studies demonstrate that EN1-iPeps were able to bind several important TFs that act as oncogenes in the mammary gland, such as PBX, Paired and Distaless family members. Our proteomics analysis also suggests that the EN1-iPeps bind a novel target, EPRS, which has been involved in the control of translation of inflammatory proteins and amino-acid stress responses, and that pharmacological inhibition of EPRS represents a potentially new treatment for basal-like breast cancer. In myeloid cells, EPRS has been shown to be a critical component of the interferon-γ-activated inhibition of translation (GAIT) complex, which controls transcript-specific translation of inflammatory gene expression.[51–53] Future research will be necessary to investigate the exact mechanism of action of the iPeps by mapping the sites of interaction and the effect on the activity on EPRS and downstream effectors in the cancer cells.

In summary, our work demonstrates that EN1 is overexpressed exclusively in basal-like breast cancers, where it has a role in

promoting survival and resistance to chemotherapy. As basal-like breast cancers are enriched in cancer stem/progenitor cell signatures,[24,54] we propose that EN1 might represent a potential novel biomarker for these cancer stem/progenitor cells. Furthermore, iPeps can be further developed and used to treat recalcitrant cancers and to sensitize tumor cells to chemotherapy and other treatments. Our work suggest that iPeps represent customable agents that could be similarly tailored to inhibit other TFs overexpressed in other cancer types in the near future, such as EN2, and even other TF families that require highly conserved and cooperative protein–protein partnerships for biological activity.

MATERIALS AND METHODS

Lentivirus preparation and transduction of breast cell lines
Plasmids expressing the EN1 cDNA (vector EX T1021-Lv107, Genecopoeia, Rockville, MD, USA) or EN1 shRNAs (Thermo Scientific, Pittsburgh, PA, USA) were transfected with Gagpol-, VSVG- and RSV-REV-coding plasmids in HEK 293T cells using Lipofectamine and Plus Reagent cationic lipids (Invitrogen, Carlsbad, CA, USA) and transduction of breast cells was performed as described.[20]

EN1 expression and prediction of relapse-free survival
To estimate the expression of EN1 across the intrinsic molecular subtypes of breast cancer, we calculated the mean expression of EN1 in the entire median centered UNC337 patient database using the subtype calls described in Prat et al.[24] Relapse-free survival was calculated using MERGE-550 database.[55]

Quantitative real-time PCR
The quantitative RT–PCR reaction was performed with TaqMan Fast Universal Master Mix (Applied Biosystems, Carlsbad, CA, USA) as described.[56]

Immunofluorescence
Tumor tissue sections were obtained from the Tissue Procurement Facility of the UNC Lineberger Comprehensive Cancer Center (Chapel Hill, NC, USA). Sections were incubated with antibodies as described.[56] HUMECs and other cultured cells were incubated at 4 °C overnight with primary antibodies (anti-EN1 (Abcam, Cambridge, MA, USA), anti-vesicular monoamine transporter (Millipore, Billerica, MA, USA), anti-dopamine transporter (Millipore), Anti-Tyrosine Hydroxylase (Millipore) and neuron-specific class III beta-tubulin (Tuj1, Abcam) diluted 1:250 and imaged using Zeiss 510 Meta Inverted Laser Scanning Confocal Microscope, Jena, Germany.

Peptide and drug treatment
All peptides were synthetized at the UNC High-Throughput Peptide Synthesis and Array Facility, Chapel Hill, NC, USA at UNC. Taxol, rotenone and halofuginone (Sigma-Aldrich, St Louis, MO, USA) were dissolved in dimethylsulfoxide. A total of 8000 or 3000 breast cells for peptide and drug treatment, respectively, were seeded in 96-well plates. Cells were exposed for 8 h to the peptide and 48–72 h for drug treatment. The cell viability after peptide/drug treatment was assayed with the CTG assay (Promega, Madison, WI, USA).[56]

Caspase-3 detection and DNA fragmentation assays
Apoptosis was detected with a Caspase-3 colorimetric assay (Sigma-Aldrich) according to the manufacturer's instructions. The quantification of DNA fragmentation was performed with a terminal deoxynucleotidyl transferase dUTP nick-end labeling assay (Millipore) and by a Hoechst 33342 staining (Sigma-Aldrich).

Immunoprecipitation/western blotting
The iPep624 and iPep624ΔHEX were coupled to a C-terminal biotin and immobilized in streptavidin-coated beads. SUM149PT protein extract (500 μg) was incubated with 20 μl of iPep-beads for 2 h with tumbling and the beads were washed three times with phosphate-buffered solution. The supernatant was removed, and the beads were boiled and loaded onto a 12% SDS–PAGE gel. The immunoprecipitations were blotted and probed with antibodies specific for PAX6, DLX6, PBX1, PBX2 and PBX3 (Santa Cruz Biotechnology, Dallas, TX, USA). Detection was performed with ECL Detection System (GE Healthcare, Pittsburgh, PA, USA) and quantitated using Image J version 1.46 (ImageJ; NIH, Bethesda, MD, USA).

Mass spectrometry/identification of EPRS
Proteins were eluted from the streptavidin beads coated with biotinylated iPep624 or iPep624ΔHEX, resuspended with SDS–PAGE sample buffer and applied to SDS–PAGE (10% acrylamide; Figure 6a). Gels were stained with Coomassie brilliant blue and select bands unique to the EN1 immunoprecipitates were excised, digested with trypsin and the peptides were extracted and analyzed using a matrix-assisted laser desorption/ionization-time of flight/time of flight mass spectrometer (AB Sciex, Framingham, MA, USA; 4800 Plus). Mass spectrometry spectra were obtained in reflector positive ion mode and peaks with signal-to-noise ratio above 10 were selected for MS/MS analysis (maximum of 45 tandem mass spectrometry spectra per spot). All spectra were searched using GPS Explorer, Version 3.6 (AB Sciex) linked to the Mascot (Matrix Science Inc., Boston, MA, USA) search engine and a Human IPI database was used.

Gene expression microarrays
The stable cell lines SUM149PT-EGFP and SUM149PT-EN1 (N = 3) were used for gene expression analyses. RNA was purified, amplified, labeled and hybridized[57] using Agilent 4 × 44K oligo microarrays (Agilent Technologies, Santa Clara, CA, USA; platform GPL10481). The probes/genes were filtered by requiring the lowest normalized intensity values in all samples to be >10. The normalized log 2 ratios (Cy5 sample/Cy3 control) of probes mapping to the same gene were averaged to generate independent expression estimates. All microarray data have been deposited in the Gene Expression Omnibus under accession number GEO: GSE47358.

REFERENCES
1 Craig DW, O'Shaughnessy JA, Kiefer JA, Aldrich J, Sinari S, Moses TM et al. Genome and transcriptome sequencing in prospective refractory metastatic triple negative breast cancer uncovers therapeutic vulnerabilities. Mol Cancer Ther 2012; 2: 104–116.
2 Rody A, Karn T, Liedtke C, Pusztai L, Ruckhaeberle E, Hanker L et al. A clinically relevant gene signature in triple negative and basal-like breast cancer. Breast Cancer Res 2011; 13: R97.
3 Shah SP, Roth A, Goya R, Oloumi A, Ha G, Zhao Y et al. The clonal and mutational evolution spectrum of primary triple-negative breast cancers. Nature 2012; 486: 395–399.
4 Creighton CJ, Li X, Landis M, Dixon JM, Neumeister VM, Sjolund A et al. Residual breast cancers after conventional therapy display mesenchymal as well as tumor-initiating features. Proc Natl Acad Sci USA 2009; 106: 13820–13825.
5 Perou CM. Molecular stratification of triple-negative breast cancers. Oncologist 2010; 15(Suppl 5): 39–48.
6 Eiro N, Fernandez-Garcia B, Gonzalez LO, Vizoso FJ. Cytokines related to MMP-11 expression by inflammatory cells and breast cancer metastasis. Oncoimmunology 2013; 2: e24010.
7 Jiang X, Shapiro DJ. The immune system and inflammation in breast cancer. Mol Cell Endocrinol 2013.
8 Rachidi SM, Qin T, Sun S, Zheng WJ, Li Z. Molecular profiling of multiple human cancers defines an inflammatory cancer-associated molecular pattern and uncovers KPNA2 as a uniform poor prognostic cancer marker. PLoS One 2013; 8: e57911.
9 Ben-Baruch A. Host microenvironment in breast cancer development: inflammatory cells, cytokines and chemokines in breast cancer progression: reciprocal tumor–microenvironment interactions. Breast Cancer Res 2003; 5: 31–36.

10 Coussens LM, Zitvogel L, Palucka AK. Neutralizing tumor-promoting chronic inflammation: a magic bullet? *Science* 2013; **339**: 286–291.

11 Kristensen VN, Vaske CJ, Ursini-Siegel J, Van Loo P, Nordgard SH, Sachidanandam R *et al.* Integrated molecular profiles of invasive breast tumors and ductal carcinoma *in situ* (DCIS) reveal differential vascular and interleukin signaling. *Proc Natl Acad Sci USA* 2012; **109**: 2802–2807.

12 Sasaki Y, Tsuda H. Clinicopathological characteristics of triple-negative breast cancers. *Breast Cancer* 2009; **16**: 254–259.

13 Cancer Genome Atlas Network. Comprehensive molecular portraits of human breast tumours. *Nature* 2012; **490**: 61–70.

14 Stephens PJ, Tarpey PS, Davies H, Van Loo P, Greenman C, Wedge DC *et al.* The landscape of cancer genes and mutational processes in breast cancer. *Nature* 2012; **486**: 400–404.

15 Nik-Zainal S, Alexandrov LB, Wedge DC, Van Loo P, Greenman CD, Raine K *et al.* Mutational processes molding the genomes of 21 breast cancers. *Cell* 2012; **149**: 979–993.

16 Gray J, Druker B. Genomics: the breast cancer landscape. *Nature* 2012; **486**: 328–329.

17 Banerji S, Cibulskis K, Rangel-Escareno C, Brown KK, Carter SL, Frederick AM *et al.* Sequence analysis of mutations and translocations across breast cancer subtypes. *Nature* 2012; **486**: 405–409.

18 Curtis C, Shah SP, Chin SF, Turashvili G, Rueda OM, Dunning MJ *et al.* The genomic and transcriptomic architecture of 2,000 breast tumours reveals novel subgroups. *Nature* 2012; **486**: 346–352.

19 Shah N, Sukumar S. The Hox genes and their roles in oncogenesis. *Nat Rev Cancer* 2010; **10**: 361–371.

20 Beltran AS, Rivenbark AG, Richardson BT, Yuan X, Quian H, Hunt JP *et al.* Generation of tumor-initiating cells by exogenous delivery of OCT4 transcription factor. *Breast Cancer Res* 2011; **13**: R94.

21 Alves dos Santos MT, Smidt MP. En1 and Wnt signaling in midbrain dopaminergic neuronal development. *Neural Dev* 2011; **6**: 23.

22 Alvarez-Fischer D, Fuchs J, Castagner F, Stettler O, Massiani-Beaudoin O, Moya KL *et al.* Engrailed protects mouse midbrain dopaminergic neurons against mitochondrial complex I insults. *Nat Neuro* 2011; **14**: 1260–1266.

23 Pandha H, Sorensen KD, Orntoft TF, Langley S, Hoyer S, Borre M *et al.* Urinary engrailed-2 (EN2) levels predict tumour volume in men undergoing radical prostatectomy for prostate cancer. *BJU Int* 2012; **110**: E287–E292.

24 Prat A, Parker JS, Karginova O, Fan C, Livasy C, Herschkowitz JI *et al.* Phenotypic and molecular characterization of the claudin-low intrinsic subtype of breast cancer. *Breast Cancer Res* 2010; **12**: R68.

25 Fan C, Prat A, Parker JS, Liu Y, Carey LA, Troester MA *et al.* Building prognostic models for breast cancer patients using clinical variables and hundreds of gene expression signatures. *BMC Med Genom* 2011; **4**: 3.

26 King MC, Marks JH, Mandell JB. Breast and ovarian cancer risks due to inherited mutations in BRCA1 and BRCA2. *Science* 2003; **302**: 643–646.

27 Jerry DJ, Kittrell FS, Kuperwasser C, Laucirica R, Dickinson ES, Bonilla PJ *et al.* A mammary-specific model demonstrates the role of the p53 tumor suppressor gene in tumor development. *Oncogene* 2000; **19**: 1052–1058.

28 Zhang M, Behbod F, Atkinson RL, Landis MD, Kittrell F, Edwards D *et al.* Identification of tumor-initiating cells in a p53-null mouse model of breast cancer. *Cancer Res* 2008; **68**: 4674–4682.

29 Wright MH, Calcagno AM, Salcido CD, Carlson MD, Ambudkar SV, Varticovski L. Brca1 breast tumors contain distinct CD44 + /CD24 − and CD133 + cells with cancer stem cell characteristics. *Breast Cancer Res* 2008; **10**: R10.

30 Wright MH, Robles AI, Herschkowitz JI, Hollingshead MG, Anver MR, Perou CM *et al.* Molecular analysis reveals heterogeneity of mouse mammary tumors conditionally mutant for Brca1. *Mol Cancer* 2008; **7**: 29.

31 Varticovski L, Hollingshead MG, Robles AI, Wu X, Cherry J, Munroe DJ *et al.* Accelerated preclinical testing using transplanted tumors from genetically engineered mouse breast cancer models. *Clin Cancer Res* 2007; **13**: 2168–2177.

32 Neve RM, Chin K, Fridlyand J, Yeh J, Baehner FL, Fevr T *et al.* A collection of breast cancer cell lines for the study of functionally distinct cancer subtypes. *Cancer Cell* 2006; **10**: 515–527.

33 Nokes BT, Cunliffe HE, Lafleur B, Mount DW, Livingston RB, Futscher BW *et al.* In vitro assessment of the inflammatory breast cancer cell line SUM 149: discovery of 2 single nucleotide polymorphisms in the RNase L gene. *J Cancer* 2013; **4**: 104–116.

34 Peltenburg LTC, Murre C. Engrailed and Hox homeodomain proteins contain a related Pbx interaction motif that recognizes a common structure present in Pbx. *EMBO J* 1996; **15**: 3385–3393.

35 Morris MC, Deshayes S, Heitz F, Divita G. Cell-penetrating peptides: from molecular mechanisms to therapeutics. *Biol Cell* 2008; **100**: 201–217.

36 Keller TL, Zocco D, Sundrud MS, Hendrick M, Edenius M, Yum J *et al.* Halofuginone and other febrifugine derivatives inhibit prolyl-tRNA synthetase. *Nat Chem Biol* 2012; **8**: 311–317.

37 Ninkovic J, Pinto L, Petricca S, Lepier A, Sun J, Rieger MA *et al.* The transcription factor Pax6 regulates survival of dopaminergic olfactory bulb neurons via crystallin alphaA. *Neuron* 2010; **68**: 682–694.

38 Morini M, Astigiano S, Gitton Y, Emionite L, Mirisola V, Levi G *et al.* Mutually exclusive expression of DLX2 and DLX5/6 is associated with the metastatic potential of the human breast cancer cell line MDA-MB-231. *BMC Cancer* 2010; **10**: 649.

39 Bell D, Bell A, Roberts D, Weber RS, El-Naggar AK. Developmental transcription factor EN1—a novel biomarker in human salivary gland adenoid cystic carcinoma. *Cancer* 2012; **118**: 1288–1292.

40 Alberi L, Sgado P, Simon HH. Engrailed genes are cell-autonomously required to prevent apoptosis in mesencephalic dopaminergic neurons. *Development* 2004; **131**: 3229–3236.

41 Morrison BE, Marcondes MC, Nomura DK, Sanchez-Alavez M, Sanchez-Gonzalez A, Saar I *et al.* Cutting edge: IL-13Ralpha1 expression in dopaminergic neurons contributes to their oxidative stress-mediated loss following chronic peripheral treatment with lipopolysaccharide. *J Immunol* 2012; **189**: 5498–5502.

42 Kim J, Byun JW, Choi I, Kim B, Jeong HK, Jou I *et al.* PINK1 deficiency enhances inflammatory cytokine release from acutely prepared brain slices. *Exp Neurobiol* 2013; **22**: 38–44.

43 Nolan YM, Sullivan AM, Toulouse A. Parkinson's disease in the nuclear age of neuroinflammation. *Trends Mol Med* 2013; **19**: 187–196.

44 Peltenburg LT, Murre C. Engrailed and Hox homeodomain proteins contain a related Pbx interaction motif that recognizes a common structure present in Pbx. *EMBO J* 1996; **15**: 3385–3393.

45 Peltenburg LT, Murre C. Specific residues in the Pbx homeodomain differentially modulate the DNA-binding activity of Hox and Engrailed proteins. *Development* 1997; **124**: 1089–1098.

46 LaRonde-LeBlanc NA, Wolberger C. Structure of HoxA9 and Pbx1 bound to DNA: Hox hexapeptide and DNA recognition anterior to posterior. *Genes Dev* 2003; **17**: 2060–2072.

47 Morgan R, Pirard PM, Shears L, Sohal J, Pettengell R, Pandha HS. Antagonism of HOX/PBX dimer formation blocks the *in vivo* proliferation of melanoma. *Cancer Res* 2007; **67**: 5806–5813.

48 Morgan R, Plowright L, Harrington KJ, Michael A, Pandha HS. Targeting HOX and PBX transcription factors in ovarian cancer. *BMC Cancer* 2010; **10**: 89.

49 Plowright L, Harrington KJ, Pandha HS, Morgan R. HOX transcription factors are potential therapeutic targets in non-small-cell lung cancer (targeting HOX genes in lung cancer). *Br J Cancer* 2009; **100**: 470–475.

50 Shears L, Plowright L, Harrington K, Pandha HS, Morgan R. Disrupting the interaction between HOX and PBX causes necrotic and apoptotic cell death in the renal cancer lines CaKi-2 and 769-P. *J Urol* 2008; **180**: 2196–2201.

51 Mukhopadhyay R, Jia J, Arif A, Ray PS, Fox PL. The GAIT system: a gatekeeper of inflammatory gene expression. *Trends Biochem Sci* 2009; **34**: 324–331.

52 Arif A, Chatterjee P, Moodt RA, Fox PL. Heterotrimeric GAIT complex drives transcript-selective translation inhibition in murine macrophages. *Mol Cell Biol* 2012; **32**: 5046–5055.

53 Yao P, Fox PL. A truncated tRNA synthetase directs a 'translational trickle' of gene expression. *Cell Cycle* 2012; **11**: 1868–1869.

54 Perou CM, Parker JS, Prat A, Ellis MJ, Bernard PS. Clinical implementation of the intrinsic subtypes of breast cancer. *Lancet Oncol* 2010; **11**: 718–719 author reply 711–720.

55 Beltran AS, Russo A, Lara H, Fan C, Lizardi PM, Blancafort P. Suppression of breast tumor growth and metastasis by an engineered transcription factor. *PLoS One* 2011; **6**: e24595.

56 Beltran AS, Rivenbark AG, Richardson BT, Yuan X, Quian H, Hunt JP *et al.* Generation of tumor initiating cells by exogenous delivery of OCT4 transcription factor. *Breast Cancer Res* 2011; **13**: R94.

57 Hu Z, Fan C, Oh DS, Marron JS, He X, Qaqish BF *et al.* The molecular portraits of breast tumors are conserved across microarray platforms. *BMC Genom* 2006; **7**: 96.

Supplementary Information accompanies this paper on the Oncogene website (http://www.nature.com/onc)